Anode Position and Last Dynode Timing Circuits for Dual-Layer BGO Scintillator with PS-PMT Based Dedicated PET Detectors

Nan Zhang, *Member, IEEE*, Christopher J. Thompson, *Member, IEEE*,
Dylan Togane, and Francois Cayouette, *Member IEEE*

***Abstract*--The new high spatial resolution PET detectors for small animal and breast imaging have been developed. In these detectors, position-sensitive photomultipliers (R7600-C12) and dual-layer pixelated BGO crystals are employed to detect and localize gamma rays. Modified high-voltage divider with last dynode readout circuits, front-end anode position and last dynode timing schemes have been investigated and developed for these detectors. Methods for combining four PS-PMTs with simple four (X^-, X^+, Y^-, and Y^+) outputs have been developed to further simplify the position processing. The front-end circuits are small so they can be fit in the detector's structure. A prototype of two detector modules, each having two PS-PMTs with corresponding electronic circuits, has been built for evaluation. The crystal elements of 10 ´ 10 in the proximal layer and 9 ´ 9 in the distal can be clearly identified.**

I. Introduction

THE high resolution, high efficiency positron emission mammography (PEM) system [1] and animal positron emission tomography (ANIPET) system [2] have been developed and constructed in Montreal Neurological Institute of McGill University. The detectors in PEM and ANIPET systems consist of bismuth germanate (BGO) crystal blocks optically coupled to Hamamatsu R3941-05 position sensitive photomultipliers (PS-PMTs). The detector field-of-view (FOV) is 56 mm × 64 mm. The timing resolution is 8.7 ns [3].

In order to improve the detector FOV and achieve better spatial resolution, we chose the small PS-PMT R7600-C12 [4] to build new high spatial resolution PEM and ANIPET detectors. Front-end position and timing electronic circuits for these new detectors have been developed. Crystal identification methods for combining both proximal and distal layer side irradiation have been investigated.

Manuscript received November 22, 2001. This work performed under a grant from the National Science and Engineering Research Council of Canada (NSERC Grant No. OPG-0036672) to Dr. Christopher J. Thompson.

N. Zhang is with McGill University, Biomedical Engineering Department, Montreal, QC H3A 2B4 Canada. (Tel: 514-398-8506, Email: nan.zhang@mail.mcgill.ca).

C. J. Thompson is with McGill University, Montreal Neurological Institute, and Biomedical Engineering Department, Montreal, QC H3A 2B4 Canada. (Tel: 514-398-8505, Email: chris@med.mcgill.ca).

D. Togane is with McGill University, Montreal Neurological Institute, Montreal, QC H3A 2B4 Canada. (Tel: 514-398-8506, Email: dtogane@hotmail.com).

F. Cayouette is with McGill University, Biomedical Engineering Department, Montreal, QC H3A 2B4 Canada. (Tel: 514-398-8506, Email: fcayouet@gel.ulaval.ca).

A. Anode Position Read-out Schemes

Many different schemes for anode readout circuits [5]-[9] are based on the fact that a PMT behaves as an almost perfect current generator - the anode current depends only on the incident flux and is completely independent of the load [10]. The common method of reading out anode signals from single PS-PMT is to combine all X or Y anode wires through a resistor divider chain. Then only four (X^-, X^+, Y^-, and Y^+) position signals output regardless of the number of anode wires. Since the PS-PMT R7600-C12 has 6 (X) + 6 (Y) anode wires, this method reduces the number of processing signals by a factor of three.

Every detector in our new PEM and ANIPET includes sixteen R7600-C12 PS-PMTs. After going through the divider chain, we still have to process 4 (X^-, X^+, Y^-, and Y^+) × 16 (PMTs) individual position signals for each detector. So it is necessary to investigate further compression methods to simplify electronics complexity. Some approaches, like combining PMTs through common X and Y resistive dividers, have been applied in the detector with multiple multi-channel PMT (MC-PMT) and PS-PMT applications [7]-[9].

We developed a new method to simplify the position circuits by combining four PS-PMTs with four (X^-, X^+, Y^-, and Y^+) position outputs. The new arrangement will reduce the number of processing signals by an additional factor of four. In the low count rate application, this method can be extended to achieve more compression by combining nine, or 16 PS-PMTs while keeping the number of outputs fixed at four.

B. Last Dynode Output from HV Divider

Typically the event-timing trigger is acquired by discriminating the energy signal from anode output. Due to the multi-anode output structure in the PS-PMT, it will simplify the electronics to take timing from one dynode output rather than from the sum of multi-anode signals.

The last dynode is chosen to take event timing because:

a. The dynode signal is synchronous with anode output so it can be chosen for anode timing measurement [10].
b. The signal taken from the last dynode has an amplitude comparable with that from the anode. It has a higher signal-to-noise ratio than the other dynodes.

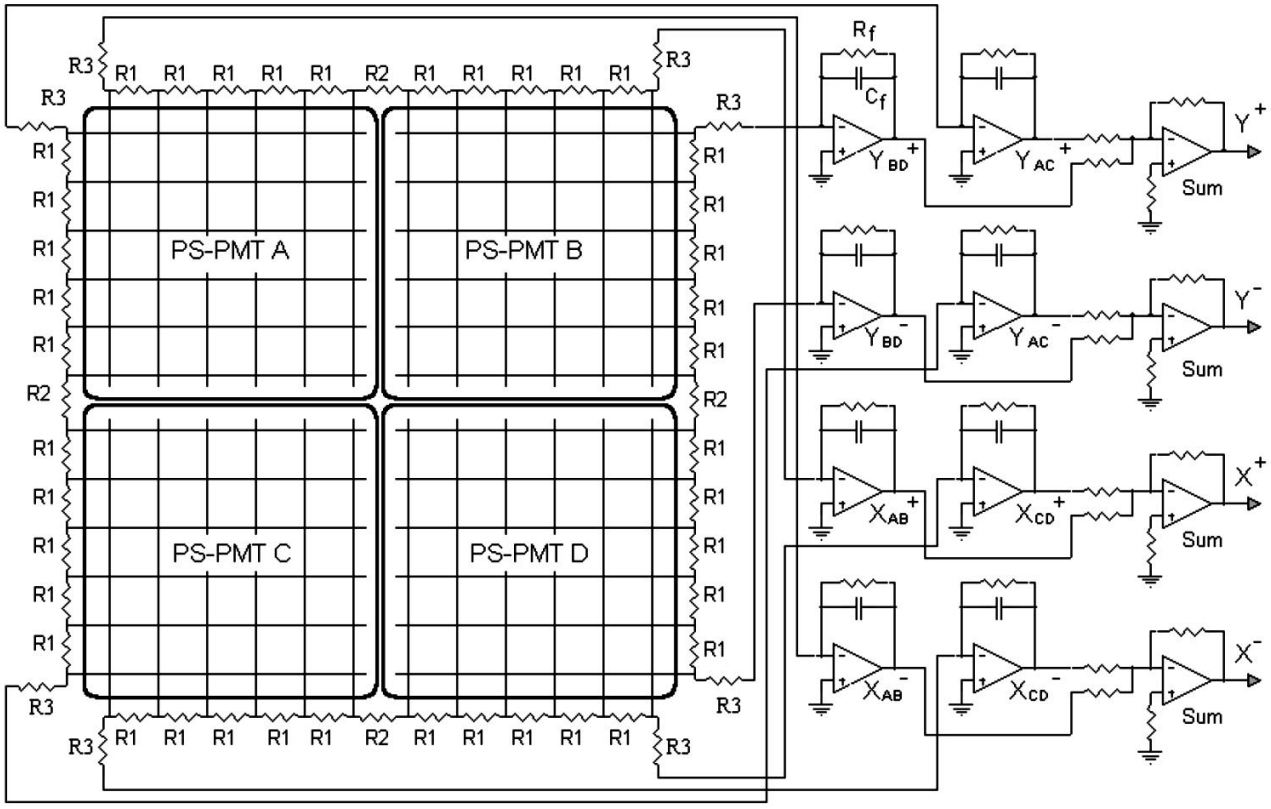

Fig. 1. Four PS-PMTs are combined together to build up as one block to further simplify the position read-out circuits. All R1 resistors are 100Ω, R2 are 20Ω, and R3 are 70Ω. The charge sensitive preamplifiers are LT1880.

C. *Fast-Slow Preamplifier Design*

The fast-slow preamplifier design is generally used in PET front-end electronics. The slow circuits are for position locating by integrating the anode outputs up to 800 ns in BGO scintillator applications [11]. The fast circuits are for timing processing to trigger the possible coincidence event.

The position preamplifiers usually employ wideband JFET input operational amplifiers because of their reduced input bias current. When precision is required, JFET amplifiers are generally inadequate due to their relatively higher input offset voltage and drift [12]. Based on this consideration, we use high precision voltage-feedback amplifiers (VFAs) in the position charge sensitive preamplifier circuits.

In order to quickly respond to the event timing, we chose the high bandwidth and ultra-fast setting time current-feedback amplifiers (CFAs) in our timing amplifier circuits. Compared with VFAs, CFAs have very low inverting input impedance so are less effected by inverting input capacitance [13]. This specification meets our needs because we know the phase shift caused by the PMT capacitance is often a source of instability.

II. Materials and Methods

The front-end electronics in our new detectors include crossed anode read-out circuits, modified HV divider, position preamplifier circuits with VFAs, and timing preamplifier circuits with CFAs.

A. *Position Read-out Configuration*

Each detector module with 2 × 2 PS-PMTs has individual position circuits. Fig. 1 illustrates the schematic for a module with four PS-PMTs (A, B, C, and D). The multi-anode wires of PS-PMTs A and B (C and D) are combined through common X resistive dividers. The anode wires of PS-PMTs A and C (B and D) are combined through common Y dividers. Eight charge sensitive preamplifiers integrate the output signals from each end of resistor chain. After four sum circuits, we have four (X^-, X^+, Y^-, and Y^+) outputs for position identification.

For example, one γ ray event happens in a crystal element faced to PS-PMT A. Four integrators (X_{AB}^-, X_{AB}^+, Y_{AC}^-, and Y_{AC}^+) will give position signals; another four integrators (X_{CD}^-, X_{CD}^+, Y_{BD}^-, and Y_{BD}^+) stay at the background level (with electronic noise). A final position signal (for example, X^+) is the sum of signal (X_{AB}^+) with background noise (X_{CD}^+). In order to achieve a high signal-to-noise ratio, the sum amplifiers are placed after the integrators.

The event position can be located by:

$$X = \frac{X^+ - X^-}{X^+ + X^-} \qquad Y = \frac{Y^+ - Y^-}{Y^+ + Y^-} \tag{1}$$

Eight integrators (X_{AB}^-, X_{AB}^+…) in Fig. 1 are charge sensitive preamplifiers. Each of them is the classical second

order model with a fast VFA, a feedback resistor R_f, and a charge storage capacitor C_f. The output voltage magnitude (V_M) of the charge sensitive amplifier is:

$$Vm \approx Q/C_f \tag{2}$$

Q is input charge with:

$$Q = \int_0^{t_w} i_t \cdot dt \tag{3}$$

where i_t is current output from the PMT anode, and t_w is the signal duration time. The feedback resistor R_f (~ 1MΩ) discharges C_f (~ 1.2pF) in continuous operation. R_f also gives the DC negative feedback to stabilize DC working points.

Only VFAs are suitable for integrating purposes. The low bias current, high precision VFAs CLC420 and the latest LT1880 [12] have been tested for our integrator circuits.

B. Last Dynode Timing Output Setup

The Hamamatsu HV divider for R7600-C12 PS-PMT was modified in order to read out a signal from the last dynode for event timing. Fig. 2 shows the schematic.

The main problem with this modification is how to obtain the signal from the last dynode without disturbing the anode signals. Compared with the manufactured HV divider circuit, three 0.01μF decoupling capacitors were changed from series decoupling to parallel. When 50Ω characteristic impedance coaxial cable is selected to transmit the dynode signal, a resistor of 200Ω to 300Ω (200Ω in Fig. 2) should be connected before dynode output. Because the last dynode still has about negative 30V voltage potential, a high voltage capacitor (0.02μF in Fig. 2) is used to AC couple the dynode output. The signal from the dynode has opposite polarity with that from the anode.

The CFA CLC450 (shown in Fig. 3 as transimpedance amplifier) was chosen to convert dynode current output to a fast response voltage signal. Compared with VFA, CFA with transimpedance setting gives a signal with a faster leading edge so it is ideal for accurate timing. Another important feature of CFA is that its inverting input impedance is very small. So CFA has much less sensitivity to inverting input capacitance [13]. With transimpedance setting (inverting mode as I/V converter), CFAs are suited to compensate the capacitance from PMT output. In practice, a small value feedback capacitor C_f between 1.0pF to 5.0pF is used to compensate for PS-PMT output capacitance.

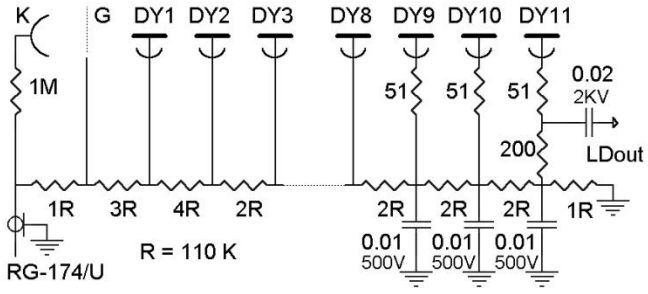

Fig. 2. This is the modified divider circuit. LDout is the last dynode output.

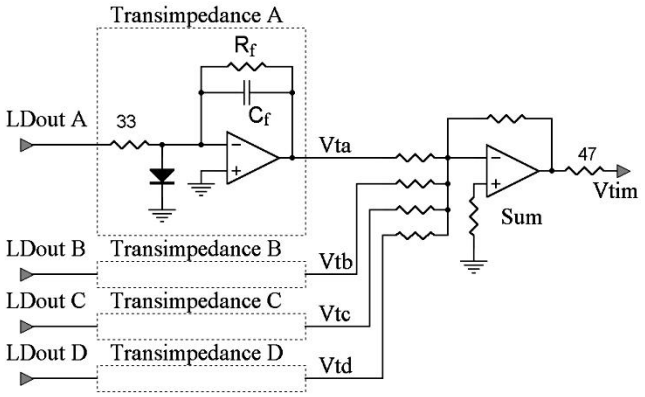

Fig. 3. This is schematic of timing amplifiers with transimpedance configuration. Sum and buffer amplifier is CLC420.

As shown in Fig. 3, each current output (LDout A, B, C, and D) from a PS-PMT last dynode is converted to a voltage signal (Vta, Vtb, Vtc, and Vtd) after the transimpedance amplifiers. The timing trigger (Vtim) of one detector module is simply the sum of these four voltage outputs.

Combining this timing scheme with position read-out arrangement, one detector module with four PS-PMTs looks exactly like a four times larger PS-PMT - it has four (X^-, X^+, Y^-, and Y^+) position and one timing outputs.

C. Detector Array, Module, and Unit Configuration

Pileup effect with a number of PS-PMTs combination [9] is one issue we have to consider in our detector structure design. Because our BGO scintillation crystal has the complex dual-layer structure, the readout circuits should be capable of identifying all crystal elements. So the detecting position accuracy is another issue we are concerned with. Fig. 4 shows our detector array, module, and unit structure.

The PEM or ANIPET system is constructed with two detector arrays. Each detector array is divided into four ideal modules. Each module consists four detector units. The basic detector unit is designed as a “field-replaceable-unit”.

Each detector module has its own position and timing electronic circuits with (X^-, X^+, Y^-, and Y^+) and a timing trigger output. Each module in one detector array can have coincidence with any module in another detector array. The coincidence events in different module pairs can be processed simultaneously.

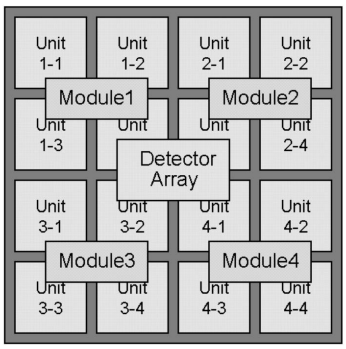

Fig. 4. This is configuration map of one detector array. Each array has four modules. Every module has four detector units.

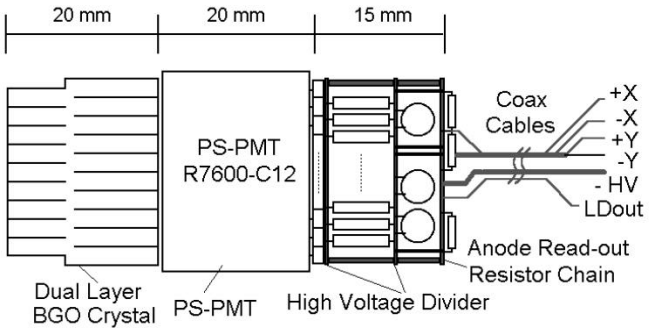

Fig. 5. This is the stack up layout of one detector unit. Two circuit boards with connecting resistors and capacitors function as the high voltage divider. The layout is roughly to scale. The length of one unit is about 55 mm (before coax cables).

An individual detector unit is shown in Fig. 5, which includes a BGO dual-layer crystal, PS-PMT R7600-C12, the HV divider, and the anode read-out resistor chain circuits.

D. Circuit Performance Evaluation

The Spice simulation software "Circuit Simulator" (an enhanced version of Berkeley SPICE3f5/Xspice) which is embedded in Protel 99/SE has been applied to verify the schematic design. The printed circuit boards for two detector modules have been built and tested.

A side irradiation method has been applied to evaluate the performance of position and timing circuits. Fig. 6 illustrates the side irradiation setup. Two kinds rod source, ^{137}Cs (622 keV) and ^{68}Ge (511 keV), are chosen for side irradiation experiments. The rod source is aligned by two lead bricks to irradiate only the proximal or distal elements of the BGO crystal block.

The list mode data with 12 bits digitized (X^-, X^+, Y^-, and Y^+) were acquired to generate spatial distortion 2D images and energy spectra for circuit performance evaluation.

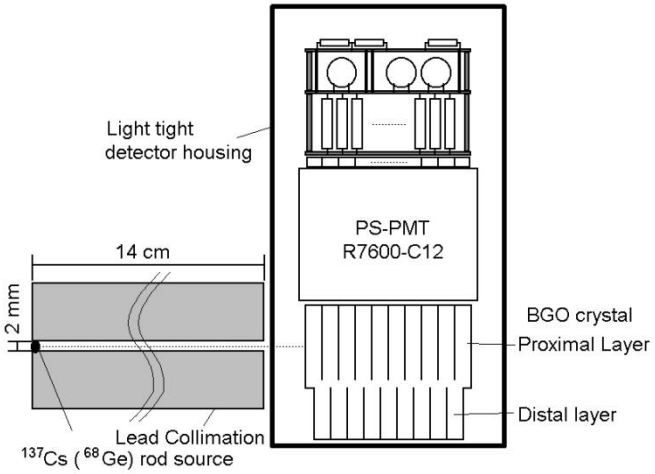

Fig. 6. The ^{137}Cs (or ^{68}Ge) rod source is aligned to irradiate only the proximal layer crystal elements (shown in the figure) or distal layer elements.

III. RESULTS

The crystal identification images (Fig. 7-A) were acquired by irradiating the crystal proximal layer (closest to the PMT) with a collimated rod source (^{137}Cs). An intensity profile (Fig. 7-C) along the white horizontal spline (Fig. 7-A) shows clear separation of the crystal elements. Fig. 7-B shows the image of the distal layer (far from the PS-PMT) with the same irradiation setup. Fig. 7-D displays the profile along the white horizontal spline (Fig. 7-B). Total crystal elements 10×10 in the proximal layer and 9×9 in the distal layer can be identified. The average peak to valley ratio of proximal layer is 4.41. It is 1.99 for the distal layer.

The energy spectra of crystal block's proximal layer (solid line) and distal layer (dashed line) with ^{137}Cs rod source are shown in Fig. 8. The spectra of two crystal elements, one from the proximal layer (white circle in Fig. 7A) and another from the distal layer (in Fig. 7B) are shown in Fig. 9.

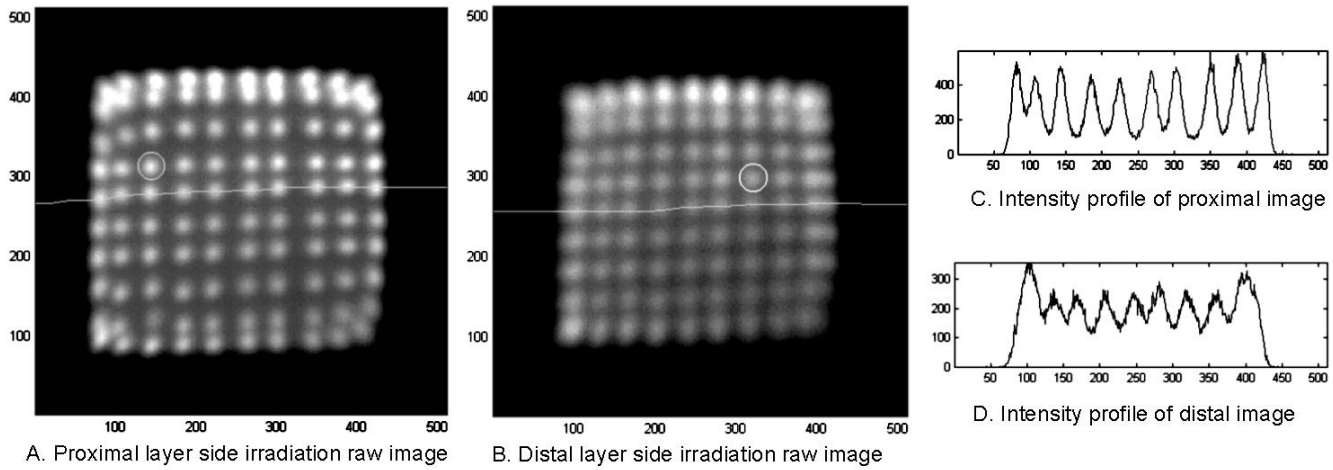

Fig. 7. These are BGO crystal side irradiation raw images and corresponding intensity profiles. The proximal 2D image (A) shows that 10×10 crystal elements can be clearly identified. The distal 2D image (B) shows that 9×9 crystal elements can be identified. The intensity profile (C) is from the white horizontal spline in the proximal image (A). The lower intensity profile (D) is from the white horizontal spline in the distal image (B).

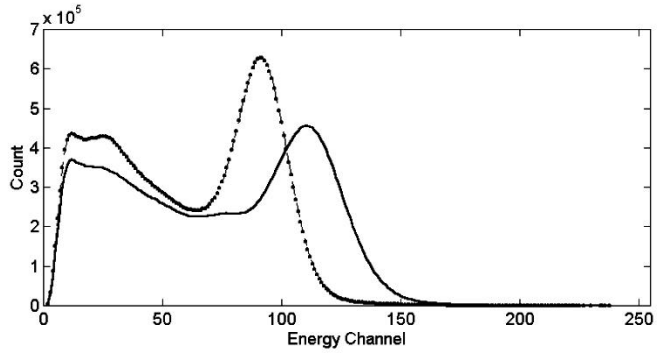

Fig. 8. Energy spectra resulting from irradiating the proximal layer (solid) and the distal layer (dashed) for the whole block with a ^{137}Cs source.

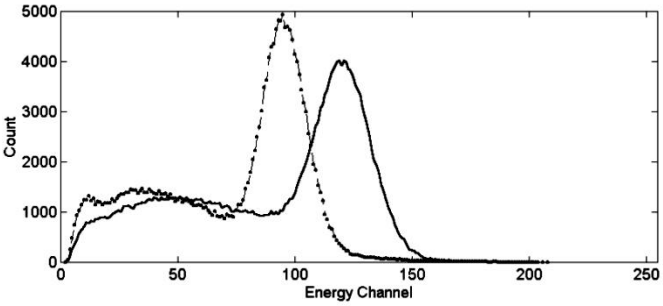

Fig. 9. Energy spectra resulting from irradiating the proximal layer (solid) and the distal layer (dashed) for the two individual crystal elements (shown in Fig. 7) with a ^{137}Cs source.

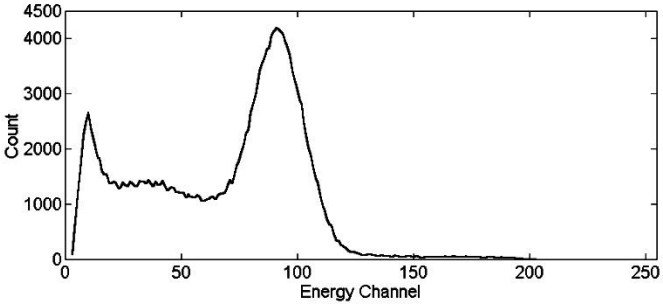

Fig. 10. Energy spectrum resulting from irradiation the proximal layer for one crystal element with a ^{68}Ge source.

The relative energy resolution of the proximal layer element (FWHM/Peak) is 20.1 %. About 61.9 % of its total counts fall in the photo peak region. The relative energy resolution of the distal layer element is 20.5 %. The counts in its photo peak area are about 62.4 % of the total.

The experiments with same setting (Fig. 6) but using ^{68}Ge source gave similar results. Fig. 10 is the energy spectrum of one crystal element in the proximal layer. The relative energy resolution is about 29.4. Photo peak counts are about 63.2 %

IV. Discussion

It is very important in PEM scanners to make the sensitive area of the detector extend to their physical edges. This allows improved imaging near the patient chest wall, and the detectors to be packed without gaps in the sensitive area. So far we chose axial through-hole resistors and HV ceramic disc capacitors to build our HV divider circuits. The axial distances can be shortened by applying surface mount resistors and capacitors.

A method of combining four PS-PMTs has been proposed. With the tradeoff potential of more pileup effects, the circuits simplify the electronic processing signals. One consideration in our circuit is to modify the charge sensitive preamplifiers. The discharge resistor R_f (Fig. 1) generally is very big so the falling edge of integrator output is slow with timing constant around 1μs. We will try other discharge schemes such as applying an analog switch [11], using an additional non-inverting low-gain amplifier [14] in future experiments.

V. Acknowledgment

This work performed under a grant from the National Science and Engineering Research Council of Canada (Grant No. OPG-0036672) to Dr. Christopher J. Thompson.

VI. References

[1] C. J. Thompson, K. Murthy, Y. Picard, I. N. Weinberg, R. Mako, "Positron Emission Mammography (PEM): A Promising Technique for Detecting Breast Cancer," *IEEE Trans. Nucl. Sci.*, vol. 42, pp. 1012-1017, 1995.

[2] C. J. Thompson, P. Sciascia, K. Murthy, S. Kecani, L. Nikinnen, E. Campo, J-F. Corbett, Y. Bercier, M. Diksic, P. Cumming, "ANIPET: a Versatile PET Scanner for Imaging Small Animals," *IEEE Nucl. Sci. Symp. Conference Record*, vol. 2, pp. 1264 -1267, 1998.

[3] N. Zhang, C. J. Thompson, C. L. Thompson, K. Nguyen, "Improving the performance of small planar detectors for dedicated PET," *IEEE Nucl. Sci. Symp. Conference Record*, vol. 3, pp. 17_51-17_57, 2000.

[4] S. Nagai, M. Watanabe, H. Shimoi, H. Liu, Y. Yoshizawa, "A new compact position-sensitive PMT for scintillation detectors," *IEEE Trans. Nucl. Sci.*, vol. 46, pp. 354 -358, Jun 1999.

[5] H. O. Anger, "Scintillation Camera," *Rev. Sci. Instr.* vol. 29, pp. 27-33, 1958.

[6] H. Kume, S. Muramatsu, M. Iida, "Position sensitive photomultiplier tubes for scintillation imaging," *IEEE Trans. Nucl. Sci.*, vol. 33, pp. 359-363, 1986.

[7] S. Siegel, R. W Silverman, Y. Shao, S. R. Cherry, "Simple charge division readouts for imaging scintillator arrays using a multi-channel PMT," *IEEE Trans. Nucl. Sci.*, vol. 43, pp. 1634-1641, Jun 1996

[8] N. K. Doshi, R. W. Silverman, Y. Shao, S. R. Cherry, "maxPET: a dedicated mammary and axillary region PET imaging system for breast cancer," *IEEE Trans. Nucl. Sci.*, vol. 48, pp. 811-815, June 2001.

[9] J. Seidel, J. J. Vaquero, F. Barbosa, I. J. Lee, C. Cuevas, M. V. Green, "Scintillator identification and performance characteristics of LSO and GSO PSPMT detector modules combined through common X and Y resistive dividers," *IEEE Trans. Nucl. Sci.*, vol. 47, pp. 1640 -1645, Aug. 2000.

[10] Philips photonics, "Photomultiplier tubes: principles & applications," pp. 5.19, 5.21, 1994

[11] H. Li, W. H. Wong, N. Zhang, J. Wang, J. Uribe, H. Baghaei, S. Yokoyama, "Electronics for a prototype variable field of view PET camera using the PMT-quadrant-sharing detector array," *IEEE Trans. Nucl. Sci.*, vol. 46, pp. 546 -550, Jun 1999.

[12] G. Brisebois, "LT1880 SOT-23 superbeta op amp saves board space in precision applications, design note 266," Linear Technology Corp., 2001.

[13] W. Kester, "High speed design techniques, Section 1: High speed operational amplifiers," Analog Device Inc. pp. 18, 1996.

[14] A. Pullia, R. Bassini, C. Boiano, S. Brambilla, "A cold discharge mechanism for low-noise fast charge amplifiers," *IEEE Trans. Nucl. Sci.*, vol. 48, pp. 530-534, June 2001.